

Soil Erosion and Land Degradation in Rural Environment: A Preliminary GIS and Remote-Sensed Approach

Giuseppe Cillis[1(✉)], Gabriele Nolè[1(✉)], Antonio Lanorte[1(✉)], Valentina Santarsiero[1,2(✉)], Biagio Tucci[1(✉)], Francesco Scorza[2(✉)], and Beniamino Murgante[2(✉)]

[1] IMAA-CNR, C.da Santa Loja, Zona Industriale, Tito Scalo, Potenza, Italy
{giuseppe.cillis,gabriele.nole,antonio.lanorte,
valentina.santarsiero,biagio.tucci}@imaa.cnr.it
[2] School of Engineering, University of Basilicata, Viale dell'Ateneo Lucano 10, 85100 Potenza, Italy
{valentina.santarsiero,francesco.scorza,
beniamino.murgante}@unibas.it

Abstract. The processes of land transformation related to soil erosion and land degradation are complex phenomena that require an approach as detailed and multidisciplinary as possible. In some Mediterranean inland areas, these issues seem to be very connected to the dynamics of transformation and abandonment of agricultural areas. In order to carry out this preliminary investigation for the assessment of dynamics and relationships between processes and land cover, an approach based on GIS and remote sensing has been applied. The study started with implementation of the Revised Universal Soil Loss Equation (RUSLE) model to calculate soil erosion on a monthly and annual basis. The resulting data were then processed through a Getis-Ord local autocorrelation index in order to produce a persistent erosion map. All datasets created were correlated with the cover classes that need more attention, i.e., arable land and post-cultivation vegetation area. All the techniques and methodologies, have been applied in a rural area of the Basilicata Region (South Italy) using exclusively a Free and Open Source Software (FoSS) GIS approach as it guarantees the possibility to perform a series of complex analyses in a simple and effective way so that they can be implemented in environmental monitoring actions and plans.

Keywords: Land degradation · RUSLE · FoSS GIS

1 Introduction

Nowadays, land degradation is one of the problems causes major consequences from an environmental point of view. In fact, this phenomenon triggers a series of related processes involving the alteration of water flows, loss of fertile soil, loss of natural habitats, ecosystem services and rural landscapes [9, 14, 20, 26]. In general terms, land

© Springer Nature Switzerland AG 2021
O. Gervasi et al. (Eds.): ICCSA 2021, LNCS 12954, pp. 682–694, 2021.
https://doi.org/10.1007/978-3-030-86979-3_48

degradation is a process driven by a combination of phenomena such as: aridity, soil erosion, land morphology and orography, vegetation cover, anthropogenic and climate factors [7].

One of these phenomena is soil erosion, which is due in particular, but not exclusively, to the intensity of rainfall. When short and intense rainfall affects soils without vegetation cover, runoff removes the surface layer rich in organic matter from the soil. Arid, semi-arid, and sub-humid areas with sunny exposures are generally at greater risk because they are often affected by short but intense rainfall, which instead of mitigating the effects of low rainfall, triggers erosion processes [17].

The causes of these processes are multiple but, especially in the inland areas of the Mediterranean regions, some dynamics related to agriculture have particularly influenced the degradation [1]. Specifically, agricultural overexploitation with unsustainable practices and land abandonment, are leading to alterations at the ecological level that need contextual analysis to assess medium and long-term effects. In fact, some agricultural practices, which are oriented to an over-exploitation of soils, to an excess of mechanized processing and to the use of chemistry [2], are leading to a reduction of soil quality and subsequent degradation.

The other phenomenon, i.e., the abandonment of agricultural activities and more generally of the territory, is at the attention of the scientific community as it can produce environmental and landscape impacts, as well as socioeconomic [13]. Obviously, over-exploitation and abandonment can have, in some particular territorial contexts, a close relationship. In fact, some areas may be abandoned precisely because of the problems following the excessive agricultural exploitation occurred in the past [25].

That said, the link between abandonment, soil erosion and land degradation needs in-depth methodological and technical investigation because the factors, dynamics and correlations are very varied and often divergent.

Starting from a study area located in Southern Italy (Basilicata Region) and suffering from problems of agricultural abandonment [22], land degradation [3] and soil consumption [27], GIS and remote sensing techniques were used to perform a preliminary investigation to assess the relationship between land degradation and soil erosion. After an initial statistical survey, arable land and areas with post-crop vegetation potentially susceptible to land degradation were mapped based on erosion rates estimated using RUSLE methodology and clustered using autocorrelation techniques.

Several indices of local spatial autocorrelation exist, but the one suggested by Ord and Getis [19], was used in this study. It is derived from a method of spatial autocorrelation. It is developed from a logic of point cluster analysis. In its first version, the index accounted for a relation between the number of remarks within a specified point range and the total sum of points. In a more generalized version, the index (as expressed by spatial weights) is applied to values at neighboring positions. This type of spatial clustering of soil erosion data allows us to obtain a new raster that contains in each pixel a number expressing how much it is autocorrelated to another pixel so it's possible define a persistent erosion map of the study area for the period considered.

Through the use of a Free and Open Source Software (FoSS) approach and open data freely available online, it was possible to set up a preliminary analysis in a single work environment thanks to the possibility of integrating different types of datasets and

data processing techniques. The increasing efficiency of FoSS GIS analysis techniques and the interoperability of different data represent a strong point both for the researcher and for the planner who wants to realize plans and strategies coherent with the rural environmental needs and problems. In fact, this work is part of the "MEV-CSU" project (University of Basilicata, CNR-IMAA and FARBAS) whose objective is to implement new advanced methodologies for the evaluation of land consumption related to the development processes of the settlement system, relational and natural environment of the Basilicata Region.

2 Materials and Methods

The analyses and computations were performed in an area of approximately 1554 km^2 within the Basilicata Region, including 17 municipalities included in the MEV CSU project. As shown in Fig. 1, the actual area does not include the real perimeter of all municipalities but, in this first phase of work, it has been cropped on the basis of the satellite image swath used. The area is characterized by a typical Mediterranean climate, with a pronounced bi-seasonal regime with hot and dry summers and cold-humid winters. Natural risks and anthropogenic activities make this area an interesting context of study because the combination of anthropogenic activities and anthropic activities and natural risks contribute to the establishment of degradation phenomena.

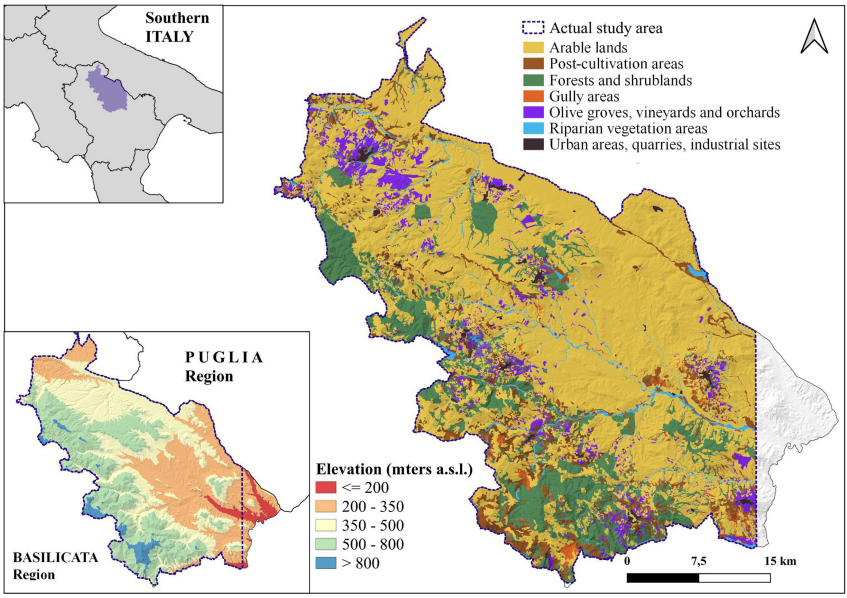

Fig. 1. Localization of study area and distribution of arable land and areas with post-cultivation vegetation.

These two categories were obtained from the Nature Map 2013 in open data format [17] aggregating some specific CORINE Biotopes classes. This dataset, although

not recently processed, was chosen instead of other open data available online after comparison and verification through photo-interpretation on current orthophotos. Mapping operation shows that arable land covers 65% of the territory and that areas with post-cultivation vegetation cover only 9%.

2.1 Monthly and Annual Erosion: RUSLE Model

The first part of work involved implementation methodologies useful for estimating and mapping areas with high erosion rates. All spatial operations were performed with QGIS 3.16 software and plugins and integrated modules of GRASS GIS and SAGA GIS; instead geostatistical operations at-through R.

One of the most widely used empirical models for soil erosion assessment is the RUSLE (Revised Universal Soil Loss Equation). The model was calculated using the following equation [23]:

$$A = R \times K \times LS \times C \times P \tag{1}$$

Where:

A = annual soil loss (Mg · ha −1 · year −1);
R = precipitation erosion factor (MJ · mm · ha −1 · h −1 · year −1);
K = soil erodibility factor (Mg · h · MJ −1 · mm −1);
LS = slope length factor and slope slope (dimensionless);
C = crop and cover management factor (dimensionless);
P = cultivation or anti-erosion (dimensionless) practice factor.

The RUSLE is based on five variables related to precipitation regime, soil properties, topography, crop cover and management, and conservation cropping practices. The result is an estimate of the amount of soil lost due to surface erosion and erosion of the rill (canalization). The parameters calculation used in previous papers [12] has been updated and modified to make the estimate more accurate.

R-factor equation is based on the rainfall intensity developed for Basilicata in the work of Capolongo [6]; in which only the daily rainfall contributions with values greater than 10 are added up.

$$R = 0.1087 * \left[\text{daily cumulated rainfall}^{(1.86)}\right]$$

The soil erodibility K-factor is the rate of soil loss per unit of the precipitation erosion index (t − ha − h − ha −1 − MJ −1 − mm −1). The calculation was based on the methodology proposed by [29]:

$$K = \left[\frac{2.1 * 10^{-4} * (12 - M) * \left[(Si + fS) * (100 - C)\right]^{1.14} + 3.25 * (A - 2) + 2.5 * (P - 3)}{100}\right] \tag{3}$$

M represents the organic matter expressed as a percentage (%) present in the soil, *Si* is the percentage of silt from 0.002–0.05 mm, *fS* the content of very fine sand with diameter 0.05–0.1 mm, and *C* the percentage of clay with diameter <0.002 mm.

The K values thus obtained, were multiplied by the factor 0.1313 in order to be expressed in the unit of the International System. For the definition of the factor on

the area of investigation the parameters were derived from the Pedological Map of the Basilicata Region and from the Basilicata region soils database [28, 29].

The formula proposed by Mitasova [15] was used to calculate the topographic LS-factor relative to a point *r*:

$$LS : (\mu + 1) * \left[\frac{a(r)}{a_0}\right]^{\mu} * x * \left[\frac{sin(b(r))}{b_0}\right]^{n} \quad (4)$$

a(r) represents the product of flow accumulation and pixel resolution (in meters) and represents the unit drained area; a_0 has a value of 22.1 m and represents the standard length defined for the calculation for USLE; b(r) is the slope in radians; b_0 has a value of 9% and represents the standard slope defined for the calculation for USLE; n was chosen to be the value 1.2 based on the work of Terranova et al. [29]. The μ value is value was calculated using formula (5) where β is the ratio of erosion type caused by flow to erosion caused by precipitation impact on soil and is equal to 0.5.

$$\mu = \frac{\beta}{\beta + 1} \quad (5)$$

The LS product factor is dimensionless and it was assumed to be constant over the entire period of observation.

The C-factor is dimensionless and is calculated to consider the impacts of vegetation cover on erosion. There are several approaches to calculation in the literature as C can vary depending on the different parameters being considered. In this work, the equation defined by Kuo et al. [11] was used:

$$C = -a * SAVI + 1 \quad (6)$$

In the Eq. (6), *a* is land cover management factor and is assumed as a value of 1.18. The *SAVI* index (Soil-Adjusted Vegetation Index) has been elaborated starting from the Sentinel-2A images. In particular, it has been used the reprocessed images of the THEIA system [31] which allows to download images already atmospherically and topographically corrected. The value of C can vary from 0 (complete vegetation cover) to 1 (no vegetation cover or bare soil).

The last factor (P) considers the effects of agricultural practices carried out to mitigate the erosion effect of rainfall. The P factor is dimensionless and values range from 0 (presence of agricultural practices for erosion mitigation) to 1 (absence of agricultural practices for erosion mitigation). The P-factor was derived from a dataset freely available online [8, 21].

All parameters calculated (Fig. 2) were resampled to spatial resolution of Sentinel-2A (10 m) and summed to get the actual value of RUSLE expressed in Mg * ha −1 * year −1.

The RUSLE values were calculated for the following months: October, November, and December 2019 and March, April, May, June, July, August, and September 2020. For the monthly RUSLEs a specific model has been implemented by Graphical Modeler of QGIS to realize a batch processing in order to calculate the different parameters in a semi-automated way. Finally, the monthly values were summed to have an annual RUSLE value. The months of January and February 2020 were not included in the calculation of RUSLE because cloudless satellite imagery is not available for C calculation.

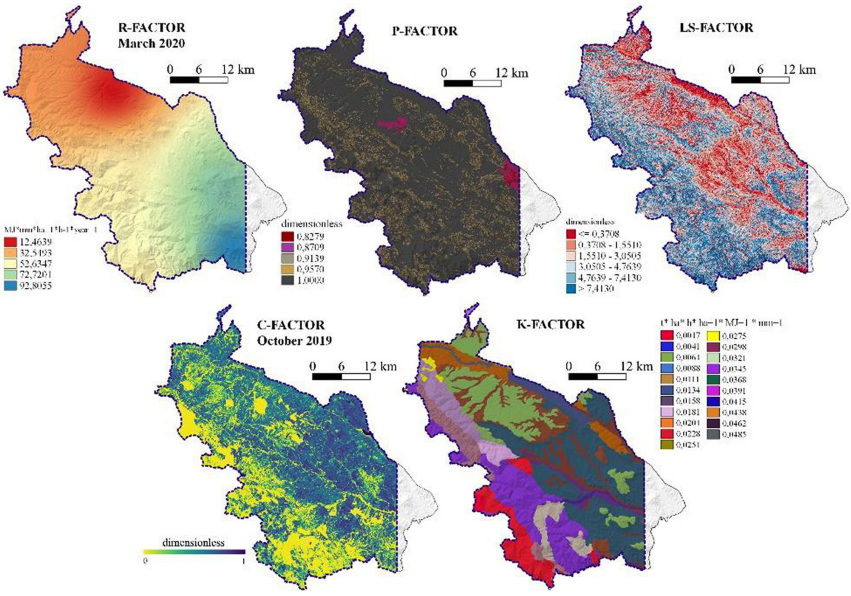

Fig. 2. The factors used to calculate RUSLE. For R and C factors, only one monthly processing each has been reported as an example.

2.2 Persistent Erosion Map

The integration of satellite imagery and geostatistical analysis is an innovative approach for analysis and mapping based on factors influenced by the spatial and geographic component. Specifically, the issue of spatial autocorrelation is fundamental to assess whether a phenomenon particularly intense in a specific area, implies the presence of the same also in contiguous areas [18]. In the present work, the autocorrelation indexes were also applied to the RUSLE model to produce a persistent erosion map.

Exploiting the potential from the R package *spdep* [4, 30], it was possible to apply several indices to the monthly RUSLE values. After several attempts, the choice fell on the G_i local autocorrelation index proposed by Ord and Getis [19].

Statistical interpretation of the index allows values to be clustered on the basis of a hot spot (pixel values greater than the mean) or cold spot (values less than the mean [23]. The index was applied individually to each month (Fig. 3) highlighting only pixels with positive autocorrelation and then subsequently cumulated into a final raster. This allowed the elaboration of a map that highlights the areas with a persistent erosion rate based on hot spot clusters.

3 Results and Discussion

The use of a FoSS and open data approach made it possible to simplify and speed up spatial analysis without losing accuracy. In addition, the possibility to integrate QGIS with R has also allowed to carry out complete geostatistical surveys reducing the workflow to a minimum. In fact, the amount of calculations and operations of the monthly

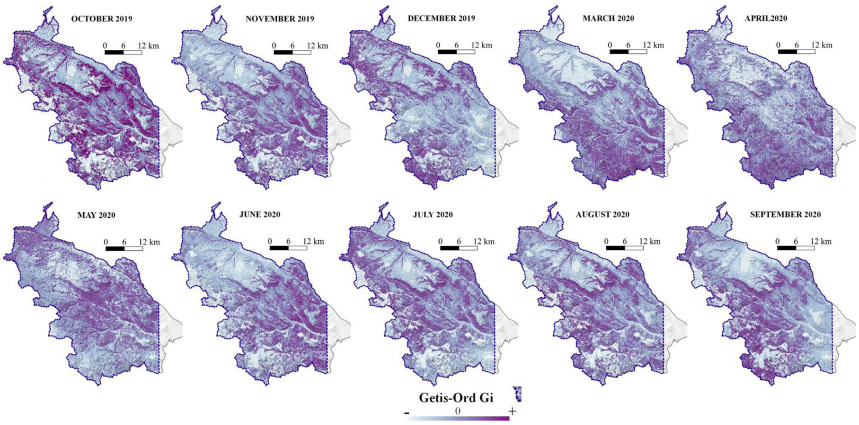

Fig. 3. Intermediate layers of Getis-Ord G_i applied to monthly RUSLEs. Values express positive or negative autocorrelation.

and annual RUSLE, was carried out quickly through the batch processing and graphical modeling features of QGIS software (Fig. 4).

The aim of this work was to relate erosion data to land cover, in order to evaluate how this process may influence degradation phenomena and the relationship between the abandonment of agricultural activities. The preliminary investigation was based on zonal statistics of average monthly and annual RUSLE values with respect to areas with arable land and post-cultivation vegetation. The data are shown in Table 1.

The analysis on annual values shows an erosion rate with same order of magnitude in two classes but with a slightly higher value in areas with post-crop vegetation. This small difference is extremely important to investigate because, generally [5] high values are noted in arable crops as they have long periods of the year with bare soil. The reason could be that the areas with post-cultivation vegetation, present a type of cover (expressed by the C-factor) and the morphological context that could influence the erosion.

From the evaluation of the arable land classes, it can be seen that the month in which the highest values are present is November 2019. This is due both to the amount of rain fallen and to the fact that November is the month in which the arable land lacks vegetative cover as it is the transition period between the end of the agricultural year and the start of sowing for the following one. for the purposes of estimating land degradation as a function of erosion, it is more useful to investigate arable land in March because in November, since there is no vegetation cover, erosion is determined, with the same erosivity of rain, only by stationary factors (R * K * LS). This is also called "Natural Potential" which does not consider the influence of vegetation. Considering that theoretically high values are unexpected, the areas in which they emerge could be indicated as those subject to a greater susceptibility to land degradation and therefore to be analysed in more detail.

On the other hand, considering the areas of post-cultivation vegetation, it can be seen that the months of greatest interest are, also in this case, November and March. November has slightly lower values than arable land, even if there is a difference in land cover in

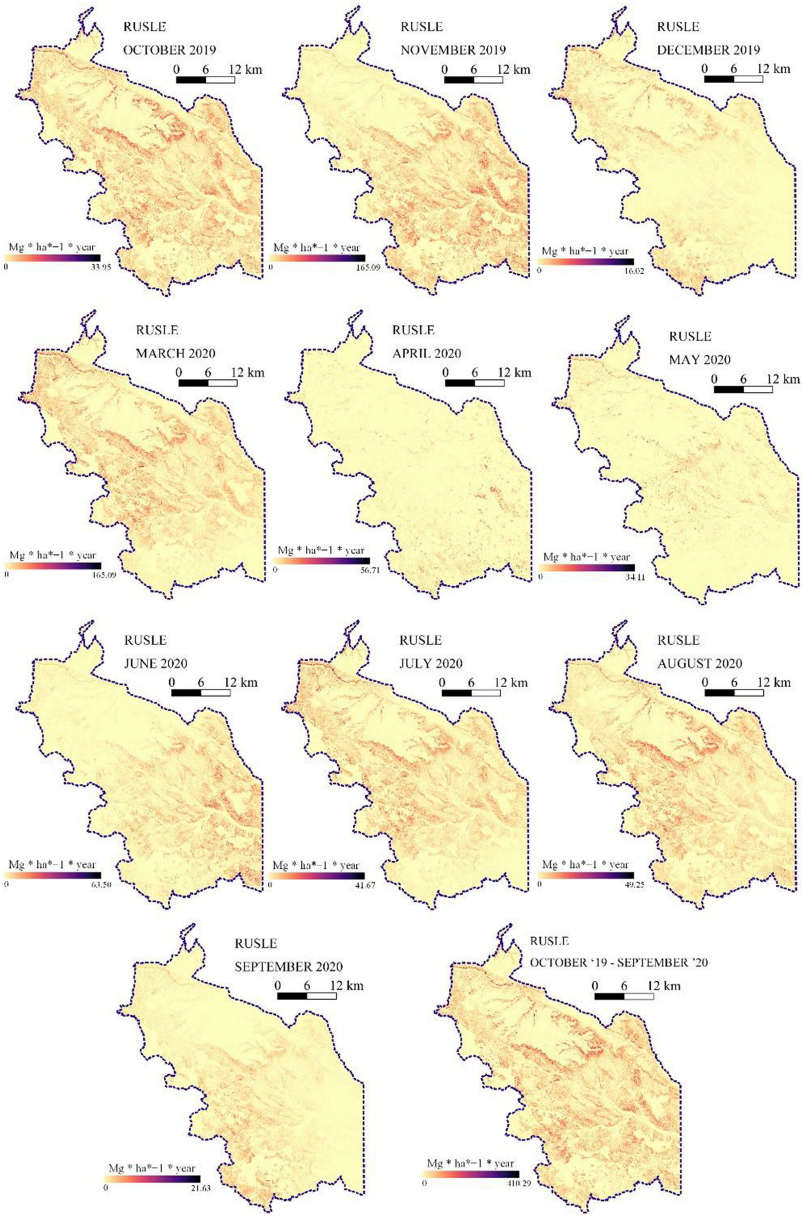

Fig. 4. Maps of monthly and annual RUSLEs expressed in Mg-ha −1 -year −1.

the two classes in this month. The reasons may be different but need a more detailed investigation as different factors could be involved, linked both to morphological and physical aspects and to different stages of abandonment. In March, on the other hand, the average value in the abandoned areas is almost double, presumably due to the fact

Table 1. Average monthly and annual RUSLE values (expressed in Mg-ha −1 -year −1) for arable lands and post-cultivation vegetation areas.

Period [Month/Year]	Post-cultivation vegetation areas	Arable lands
October '19	1.81	2.10
November '19	8.81	8.84
December '19	0.42	0.34
March '20	7.22	3.94
April '20	0.90	0.35
May '20	0.37	0.39
June '20	1.95	2.19
July '20	1.85	1.96
August '20	2.29	2.33
September '20	0.62	0.48
Year [October '19–September '20]	**26.23**	**22.92**

that in this month the arable land already provides a certain degree of ground cover and the herbaceous and shrub vegetation does not yet, since the growing season begins later than that of cereals and arable land in general.

The geostatistical operations performed through G_i local autocorrelation allowed for the creation of a persistent erosion map (Fig. 5) that takes into account the spatial and geographic relationship that may exist between contiguous areas that emerge from the calculations of monthly RUSLEs. The pixels highlighted in the map are spatially and geographically related to each other based on the intensity of the monthly RUSLE value. In this raster map, the pixels have been reclassified so that they have only discrete 0–1 values. The areas of interest are those that have a value of 1, i.e. all those areas that during all the months analyzed, have positively autocorrelated RUSLE values. This means that in these areas, there is a constant erosion contribution during all months of analysis.

Table 2 shows only some of the most important aggregate classes of land cover in order to make a comparison with the values recorded in arable land and post-cultivation vegetation areas. In addition, the zonal statistics carried out directly on QGIS allowed an immediate tabulation of the data. The other classes were derived from the Nature Map [10] as well.

The spatial statistical analysis shows that, in percentage terms, the arable land and the areas with post-cultivation vegetation are precisely those which present higher values of vegetation than the others, and that especially the latter represents more than 61%.

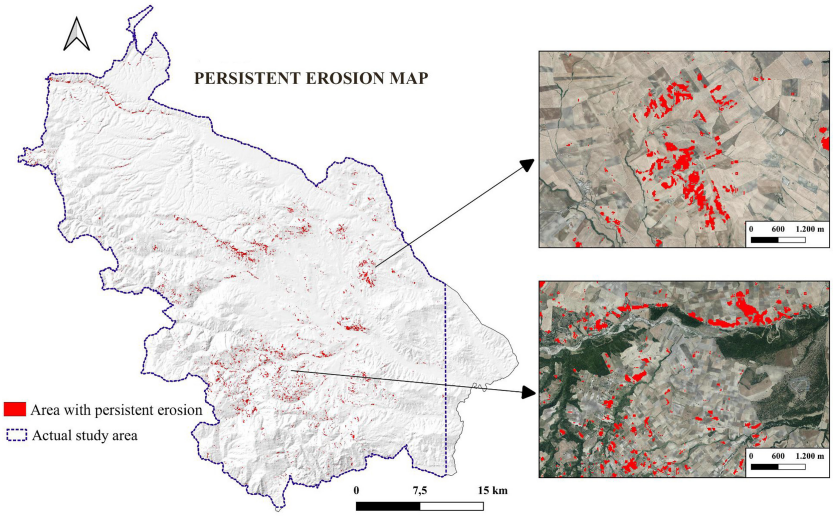

Fig. 5. In red, areas with persistent erosion estimated between October 2019 and September 2020. On the right, two details on two areas overlaid on the 2017 orthophoto.

Table 2. Table captions should be placed above the tables.

Land cover classes	Hectares (ha) in persistent erosion	% of total persistently eroded area
Arable lands	493.947	22.480
Post-cultivation vegetation area	1343.107	61.125
Olive groves, vineyards and orchards	143.895	6.549
Forests and shrublands	29.568	1.346
Riparian vegetation areas	18.518	0.843
Gully areas	149.48	6.803
Urban areas, quarries, industrial sites	18.795	0.855
Total	2197.310	100

4 Conclusion

Land degradation, defined as the loss of soil's capacity to provide ecosystem services, is a complex phenomenon that requires a multi-disciplinary approach since there are many factors that contribute to its determination. For the purpose of the objective of this study, water-related soil erosion was considered as a parameter closely related to land degradation. To do this, spatial analysis techniques based on the integration of

remote sensing data were applied in order to estimate the degradation processes starting from the implementation of the RUSLE model. The complexity of the phenomena and processes analyzed cannot ignore the use of a GIS working environment that allows the integration of basic spatial analysis, remote sensing image classification and more advanced geostatistical analysis. To do this, a FoSS approach was tested so that the workflow could be reduced and work in an interoperable way with other software without losing computational capacity. Moreover, thanks to the ease of management of different datasets, it was possible to quickly integrate other types of ancillary data in order to make the analysis more functional and detailed.

Specifically, the application of the RUSLE model on a monthly and annual basis, the use of the index of local autocorrelation *Gi* and the analysis with respect to land cover, has allowed to implement a preliminary GIS methodology useful to elaborate data necessary to enter more in detail the dynamics of land degradation. In the inland rural areas of the Mediterranean, where processes are very different, the use of GIS tools allow to carry out detailed analysis at local scale in a very effective and, in some respects, innovative way thanks to the possibility of integrating different types of data and surveys. In addition, through clustering operations, these techniques can provide useful information for spatial decision support systems (sDSS) to identify areas that are more vulnerable and need further analysis and monitoring.

References

1. Bajocco, S., Smiraglia, D., Scaglione, M., Raparelli, E., Salvati, L.: Exploring the role of land degradation on agricultural land use change dynamics. Sci. Total Environ. **636**, 1373–1381 (2018). https://doi.org/10.1016/j.scitotenv.2018.04.412
2. Basso, F., Pisante, M., Basso, B.: Soil erosion and land degradation, In: Geeson, N.A., Brandt, C.J., Thornes, J.B., (eds.) Mediterranean Desertification, a Mosaic of Processes and Responses. John Wiley & Sons, Ltd (2002)
3. Basso, B., et al.: Evaluating responses to land degradation mitigation measures in Southern Italy. Int J Environ Res. **6**(2), 367–380 (2012)
4. Bivand, R.S., Wong, D.W.S.: Comparing implementations of global and local indicators of spatial association. TEST **27**(3), 716–748 (2018). https://doi.org/10.1007/s11749-018-0599-x
5. Borrelli, P., Robinson, D.A., Fleischer, L.R., et al.: An assessment of the global impact of 21st century land use change on soil erosion. Nat. Commun. **8**, 2013 (2017). https://doi.org/10.1038/s41467-017-02142-7
6. Capolongo, D., Pennetta, L., Piccarreta, M., Fallacara, G., Boenzi, F.: Spatial and temporal variations in soil erosion and deposition due to land-levelling in a semi-arid area of Basilicata (Southern Italy). Earth Surf. Proces. Landforms: J. British Geomorphol. Res. Group **33**(3), 364–379 (2008)
7. D'Odorico, P., Bhattachan, A., Davis, K.F., Ravi, S., Runyan, C.W.: Global desertification: drivers and feedbacks. Adv. Water Resour **51**, 326–344 (2013)
8. ESDAC. https://esdac.jrc.ec.europa.eu/content/support-practices-factor-p-factor-eu. Accessed on 15 Jan 2021
9. González Díaz, J.A., Celaya, R., Fernández García, F., Osoro, K., Rosa García, R.: Dynamics of rural landscapes in marginal areas of northern Spain: past, present, and future. Land Degrad Dev. **30**, 141–150 (2019). https://doi.org/10.1002/ldr.3201
10. ISPRA. https://www.isprambiente.gov.it/it/servizi/sistema-carta-della-natura. Accessed on 14 Jan 2021

11. Kuo, K.T., Sekiyama, A., Mihara, M.: Determining C factor of universal soil loss equation (USLE) based on remote sensing. Int. J. Environ. Rural Dev. **7**(2), 154–161 (2016)
12. Lanorte, A., et al.: Integrated approach of RUSLE, GIS and ESA Sentinel-2 satellite data for post-fire soil erosion assessment in Basilicata region (Southern Italy). Geomat. Natl. Hazards Risk **10**(1), 1563–1595 (2018). https://doi.org/10.1080/19475705.2019.1578271
13. Lasanta, T., Sánchez-Navarrete, P., Medrano-Moreno, L.M., Khorchani, M., Nadal-Romero, E.: Soil quality and soil organic carbon storage in abandoned agricultural lands: Effects of revegetation processes in a Mediterranean mid-mountain area. Land Degrad Dev. **31**, 2830–2845 (2020)
14. Las Casas, G., Scorza, F., Murgante, B.: New Urban Agenda and open challenges for urban and regional planning. In: Calabrò, F., Della Spina, L., Bevilacqua, C. (eds.) New Metropolitan Perspectives. ISHT 2018. Smart Innovation, Systems and Technologies, vol. 100. Springer, Cham (2019). https://doi.org/10.1007/978-3-319-92099-3_33
15. Mitasova, H., Hofierka, J., Zlocha, M., Iverson, L.R.: Modelling topographic po-tential for erosion and deposition using GIS. Int. J. Geogr. Inf. Syst. **10**(5), 629–641 (1996)
16. Mohamadi, M.A., Kavian, A.: Effects of rainfall patterns on runoff and soil erosion in field plots Int. Soil Water Conservat. Res. **3**(4), 273–281 (2015). https://doi.org/10.1016/j.iswcr.2015.10.001
17. Nature Map. https://www.isprambiente.gov.it/it/servizi/sistema-carta-della-natura. Accessed on 10 Jan 2021
18. Nolè, G., Lasaponara, R., Lanorte, A., Murgante, B.: Quantifying Urban Sprawl with spatial autocorrelation techniques using multi-temporal satellite data. Int. J. Agric. Environ. Inf. Syst. **5**(2), 19–37 (2014). https://doi.org/10.4018/IJAEIS.2014040102
19. Ord, J.K., Getis, A.: Local spatial autocorrelation statistics: distributional issues and an application. Geogr. Anal. **27**, 286–306 (1995)
20. Pacheco, F.A.L., Sanches Fernandes, L.F., Valle Junior, R.F., Valera, C.A., Pissarra, T.C.T.: Land degradation: multiple environmental consequences and routes to neutrality. Curr. Opin. Environ. Sci. Heal. **5**, 79–86 (2018). https://doi.org/10.1016/j.coesh.2018.07.002
21. Panagos, P., Borrelli, P., Meusburger, K., van der Zanden, E.H., Poesen, J., Alewell, C.: Modelling the effect of support practices (P-factor) on the reduction of soil. Environ. Sci. Policy **51** (2015). https://doi.org/10.1016/j.envsci.2015.03.012(2015)
22. Picuno, P., Cillis, G.,Statuto, D.: Investigating the time evolution of a rural landscape: How historical maps may provide environmental information when processed using a GIS. Ecol. Eng. **139** (2019). https://doi.org/10.1016/j.ecoleng.2019.08.010
23. Peeters, A., et al.: Getis–Ord's hot- and cold-spot statistics as a basis for multivariate spatial clustering of orchard tree data. Comput. Electron. Agric. **111**, 140–150 (2015). https://doi.org/10.1016/j.compag.2014.12.011
24. Renard, K.G., Foster, G.R., Weesies, G.A., Porter, J.P.: RUSLE: revised uni-versal soil loss equation. J. Soil Water Conserv. **46**(1), 30–33 (1991)
25. Rodrigo-Comino, J., Martínez-Hernández, C., Iserloh, T., Cerdà, A.: The contrasted impact of land abandonment on soil erosion in mediterranean agriculture fields. Pedosphere (2017). https://doi.org/10.1016/S1002-0160(17)60441-7
26. Scorza, F., Casas, G.B.L., Murgante, B.: That's ReDO: Ontologies and regional development planning. In: Murgante, B., et al. (eds.) Computational Science and Its Applications – ICCSA 2012. ICCSA 2012. Lecture Notes in Computer Science, vol. 7334. Springer, Berlin, Heidelberg (2012). https://doi.org/10.1007/978-3-642-31075-1_48
27. Santarsiero, V., Nolè, G., Lanorte, A., Tucci, B., Baldantoni, P., Murgante, B.: Evolution of soil consumption in the municipality of melfi (Southern Italy) in relation to renewable energy. In: Misra, S., et al. (eds.) ICCSA 2019. LNCS, vol. 11621, pp. 675–682. Springer, Cham (2019). https://doi.org/10.1007/978-3-030-24302-9_48

28. Soils database - Basilicata Region. http://www.basilicatanet.it/suoli/carta2.htm. Accessed on 02 March 2021
29. Spdep. https://cran.r-project.org/package=spdep. Accessed on 14 Feb 2021
30. Terranova, O., Antronico, L., Coscarelli, R., Iaquinta, P.: Soil erosion risk scenarios in the Mediterranean environment using RUSLE and GIS: an application model for Calabria (southern Italy). Geomorphology **112**(3–4), 228–245 (2009)
31. THEIA Homepage. https://theia.cnes.fr/atdistrib/rocket/#/home. Accessed on 20 March 2021